Programmable CGH on photochromic material using DMD

Alata, Romain, Pariani, Giorgio, Zamkotsian, Frederic, Lanzoni, Patrick, Bianco, Andrea, et al.

Romain Alata, Giorgio Pariani, Frederic Zamkotsian, Patrick Lanzoni, Andrea Bianco, Chiara Bertarelli, "Programmable CGH on photochromic material using DMD," Proc. SPIE 9912, Advances in Optical and Mechanical Technologies for Telescopes and Instrumentation II, 991234 (22 July 2016); doi: 10.1117/12.2234406

SPIE.

Event: SPIE Astronomical Telescopes + Instrumentation, 2016, Edinburgh, United Kingdom

Programmable CGH on photochromic material using DMD

Romain Alata[1], Giorgio Pariani[2], Frederic Zamkotsian[1], Patrick Lanzoni[1],
Andrea Bianco[2], Chiara Bertarelli[3]

[1] Aix Marseille Université, CNRS, LAM (Laboratoire d'Astrophysique de Marseille) UMR 7326, 13388, Marseille, France
[2] INAF – Osservatorio Astronomico di Brera, Via Bianchi
46, 23807 Merate, Italy
[3] Politecnico di Milano, Dipartimento di Chimica, Materiali de
Ingegneria Chimica, p.zza L. Da Vinci 32, 20133, Milano, Italy

e-mail: romain.alata@lam.fr, frederic.zamkotsian@lam.fr

ABSTRACT

Computer Generated Holograms (CGHs) are useful for wavefront shaping and complex optics testing, including aspherical and free-form optics. Today, CGHs are recorded directly with a laser or intermediates masks but allows only recording binary CGHs; binary CGHs are efficient but can reconstruct only pixilated images. We propose to use a Digital Micro-mirror Device (DMD) for writing binary CGHs as well as grayscale CGHs, able to reconstruct fulfilled images. DMD is actually studied at LAM, for generating programmable slit masks in multi-object spectrographs. It is composed of 2048x1080 individually controllable micro-mirrors, with a pitch of 13.68 µm. This is a real-time reconfigurable mask, perfect for recording CGHs. A first setup has been developed for hologram recording, where the DMD is enlightened with a collimated beam and illuminates a photosensible plate through an Offner relay, with a magnification of 1:1. Our set up resolution is 2-3 µm, leading to a CGH resolution equal to the DMD micro mirror size. In order to write and erase CGHs during test procedure or on request, we use a photochromic plate called PUR-GD71-50-ST developed at Politecnico di Milano. It is opaque at rest, and becomes transparent when it is illuminated with visible light, between 500 and 700 nm; then it can be erased by a UV flash. We choose to code the CGHs in equally spaced levels, so called ***stepped CGH***. We recorded up to 1000x1000 pixels CGHs with a contrast greater than 50, knowing that the material is able to reach an ultimate contrast of 1000. A second bench has also been developed, dedicated to the reconstruction of the recorded images with a 632.8nm He-Ne laser beam. Very faithful reconstructions have been obtained. Thanks to our recording and reconstruction set-ups, we have been able to successfully record binary and stepped CGHs, and reconstruct them with a high fidelity, revealing the potential of this method for generating programmable/rewritable stepped CGHs on photochromic materials.

Key words: Computer Generated Hologram, programmable CGH, MOEMS, photochromic material, optical testing, wavefront shaping, DMD, stepped CGH.

1. INTRODUCTION

A hologram corresponds to the interference pattern between a wave coming from an object and a reference wave. Since the work of Lohmann [1, 2] in 1967, it is possible to calculate that pattern, via a computer, without needing the physical object. First used for spatial filtering [1,3,4,5], computer-generated holograms (CGHs) have been studied extensively [6], to generate discrete point holograms [7], large scale holograms [8], using Fresnel [9] and Fourier transform [10] and the number of applications has been increasing as well as the number of study on quality [11] and noise [12, 13]. Largely

Advances in Optical and Mechanical Technologies for Telescopes and Instrumentation II,
edited by Ramón Navarro, James H. Burge, Proc. of SPIE Vol. 9912, 991234
 · doi: 10.1117/12.2234406

used and studied for optical testing [14, 15], they are now present in many research areas such as image display and electronic memory and security.

There are two types of CGHs depending on how the information is encoded, and recording methods differs from one to the other: phase holograms and amplitude holograms. It is possible to encode the phase variations with a varying thickness of a material having a certain refractive index, which gives phase holograms, but we will focus on the second type of CGH in this paper, which are amplitude holograms. They can be recorded on a material whose transparency can be controlled locally. Our method of recording is based on the latter principle.

Today, amplitude holograms are recorded with hard masks done one by one illuminating the photosensitive plate through it, or directly written with a laser. These techniques allow writing binary CGHs easily, but are not suited to record a grayscale CGH, i.e. CGHs with gray levels. To our best knowledge, grayscale CGH have been used in micro-lithography with phase holograms [16], but none for amplitude holograms; the precision on the material thickness is main limiting parameter [17]. It is critical to correctly align a consecutive serial of hard masks for generating multiple gray levels; in addition this process is time consuming. The originality of our recording technique lies in the use of a micro-mirror array (DMD) that is versatile enough to record grayscale CGHs. DMDs are studied at LAM for generating programmable slit masks for a multi-object spectroscopy [18]. It consists of an array of 2048x1080 micro mirrors controlled individually, with a pitch of 13.68 µm. So these are reconfigurable masks in real time are perfect for reproducing binary patterns, thus writing CGHs onto a photosensitive plate. The material we use for that is developed at Politecnico di Milano. This is a photochromic material called PUR - GD71-50 - ST responding differently according to the light wavelength [19]. Opaque at rest, it becomes progressively transparent when illuminated by visible light. We can then read recorded information using a low power 632.8 nm laser and delete it with a UV flash. The figure 1 shows the absorbance spectrum of this photochromic material and illustrates its behavior.

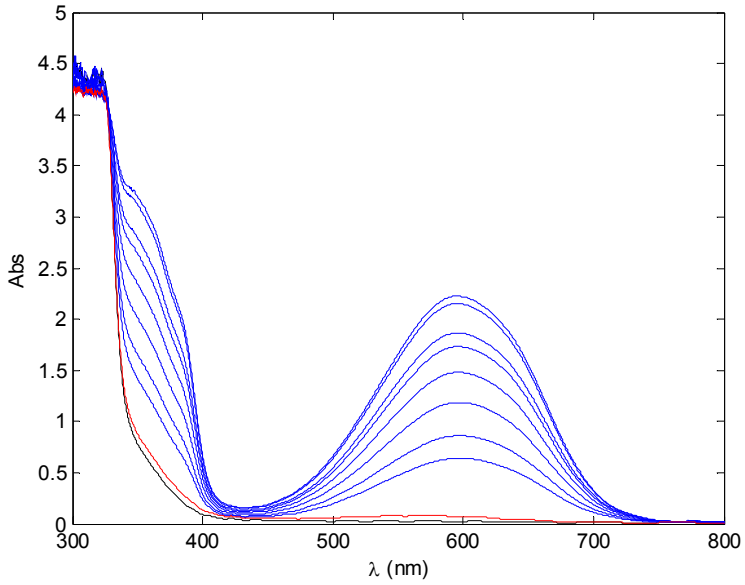

Figure 1: Absorbance of the photochromic material used in the UV-Visible range of the spectrum for different UV illumination time, from [19]

In this paper, the calculation of different types of CGHs will be presented, then the methodology used to record them will be explained. First successful stepped CGHs results will be presented. Finally, a comparison of binary and stepped CGHs will be done.

2. CGHs CALCULATION

CGHs could be calculated as Fourier holograms and Fresnel holograms. In this paper we will focus on Fresnel CGHs.

2.1 Fourier holograms

Fourier holograms are obtained using algorithms encoding the inverse Fourier transform of the wavefront to be reproduced. These algorithms [20, 21, 22] are operating in a common way. Once the inverse Fourier transform is calculated, the complex information contained in each pixel is encoded in a cell of WxH pixels, W and H depending on the used algorithm. The number of pixels of a Fourier hologram is therefore necessarily larger than the number of pixels defining the image. This leads to limitating the resolution and size of images to be encoded. The DMD is composed of 2048x1080 micro mirrors and the dimensions W and H being 4 pixels or larger, with the most compact algorithm, the maximum attainable resolution of the image to be encoded is 250x250 pixels, and its actual size is limited to 3,4x3.4mm. Since these holograms are based on the Fourier transform, it is necessary to add a lens after the CGH in the reconstruction set-up, for applying the optical Fourier transform to the CGH and display the image. Fourier holograms could be calculated very fast but they will not be discussed in this paper.

2.2 Fresnel holograms

Fresnel holograms are directly calculated with the light propagation equations, and can be modeled by the Rayleigh - Sommerfeld integral diffraction given in equation 1 [23].

$$A_z(x,y) = \frac{A_0}{i\lambda} \iint t(u,v) \frac{e^{ikr}}{r} \cos(\theta)\, dudv \tag{1}$$

The resulting complex wave A_z is estimated by calculating the sum of the contributions of each pixel of the hologram anywhere on the screen located at a distance z. Each pixel is considered as a secondary spherical wave source weighted by the transmittance t(x, y) of the hologram. These secondary waves are generated when the incident wave, characterized by its complex amplitude A_0 and its wavelength λ (or the wave number k = 2π/λ), reaches the hologram. The angle θ is the skew factor and is equal to zero in our configuration.

The distance z between the hologram and the screen being much greater than the dimensions of the detector and CGH dimensions, the equation (1) can be approximated by the following 2D convolution product :

$$A_z(x,y) = A_0(x,y) e^{ikz} t * h_z \tag{2}$$

Where the kernel convolution h_z, called Fresnel function, is :

$$h_z(x,y) = \frac{1}{i\lambda z} e^{(i\pi \frac{x^2+y^2}{\lambda z})} \tag{3}$$

The equation (2) simulates the diffraction of the reference wave on the hologram and thus reconstructs the digitally encoded image, the development of this reconstruction being obtained by estimating the convolution kernel h_z at the desired focal length z.

The convolution function is defined by the equation (4):

$$a(x,y) = \iint b(u,v).c(x-u, y-v)\, dudv = b * c \tag{4}$$

3. RECORDING AND RECONSTRUCTION OF A CGH

We developed 2 set-ups, respectively dedicated to the recording of the calculated CGH and the reconstruction of the original encoded images.

3.1 Recording set-up

Figure 2 shows our first set-up, dedicated to the CGH recording on the photosensitive plate. The DMD, controlled by the formatter board [24, 25] is illuminated by a collimated beam from a white source, and redirects the light toward the plate. The beam is illuminating the entire DMD and the light power is homogeneous at every point of the plate. The pattern reproduced by the DMD has to be projected onto the plate as precisely as possible, so the plate is illuminated through an Offner relay with a magnification of 1:1. This relay provides a nearly aberration free beam and has the advantage of being compact. The unit magnification means that the maximum size of CGH is directly limited by the size of the DMD; the micro-mirrors of the DMD therefore correspond to the "pixels" of the CGH. Finally, a post-CGH imaging system located right after the CGH plate consists of two lenses, a filter around 600 nm and a CCD camera. This system in an afocal assembly allows imaging of the CGH during writing, in situ and in real time. Magnification is tuned by changing properly the pair of lenses, from a value of 1 up to 4.

DMD, CGH and camera planes are then conjugated. Note that DMD plane is a tilted focal plane due to the nature of micro-mirror array: each micro-mirrors tilts out of the array plane by 12°, leading to a global 24° tilted focal plane. This effect is reproduced as well at the post-CGH imaging camera level (the camera plane is tilted by 24°).

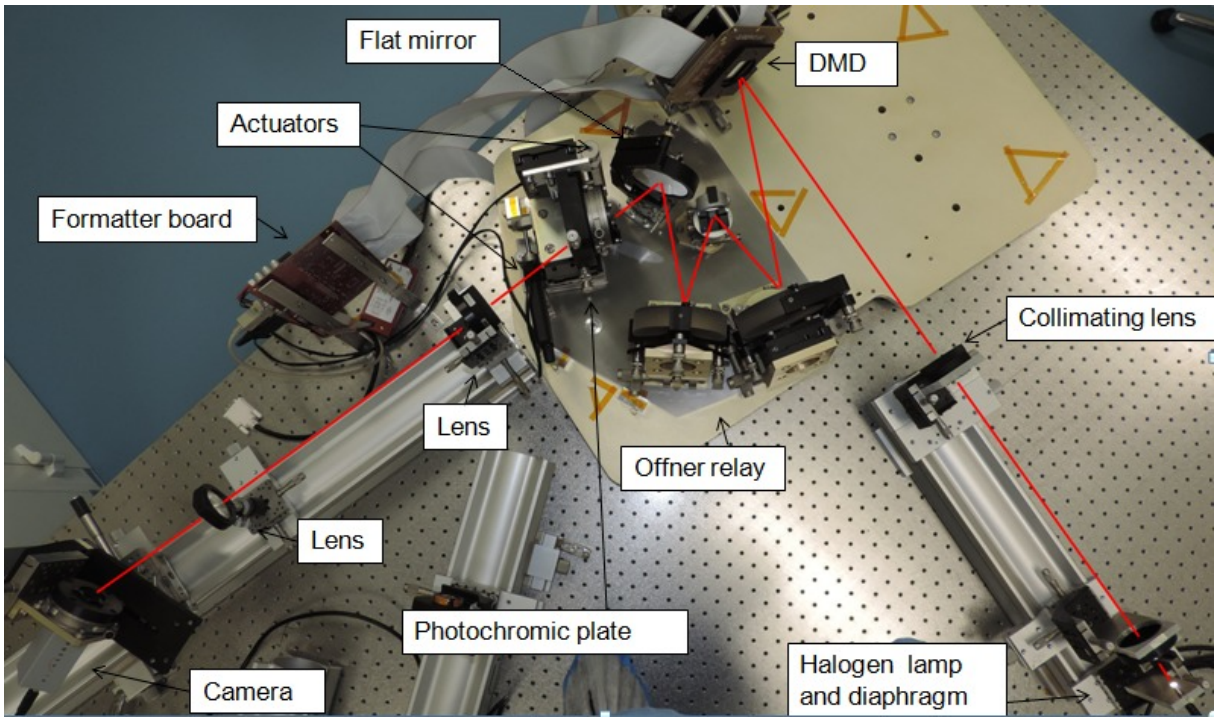

Figure 2: Picture of the set-up dedicated to CGHs recording; it is based on an illumination unit towards the DMD, an imaging optical system based on a 1:1 magnification Offner relay from the DMD plane to the CGH plane, and a post-CGH imaging system.

3.2 Reconstruction set-up

The second set-up, shown in Figure 3, is dedicated to CGH reconstruction. The source is a collimated He-Ne laser. The camera, placed at the distance z from the plate, is illuminated through the CGH. As we saw in the previous section, the Fresnel holograms are directly calculated from the propagation equations of light, and they are for a given focus. It is thus not necessary to add a lens between the plate and the camera to reconstruct the image, unlike with the Fourier holograms. This is why the source should be rigorously collimated, because a variation in the quality of the collimation can displace the focal plane along the optical axis and change the size of the encoded image.

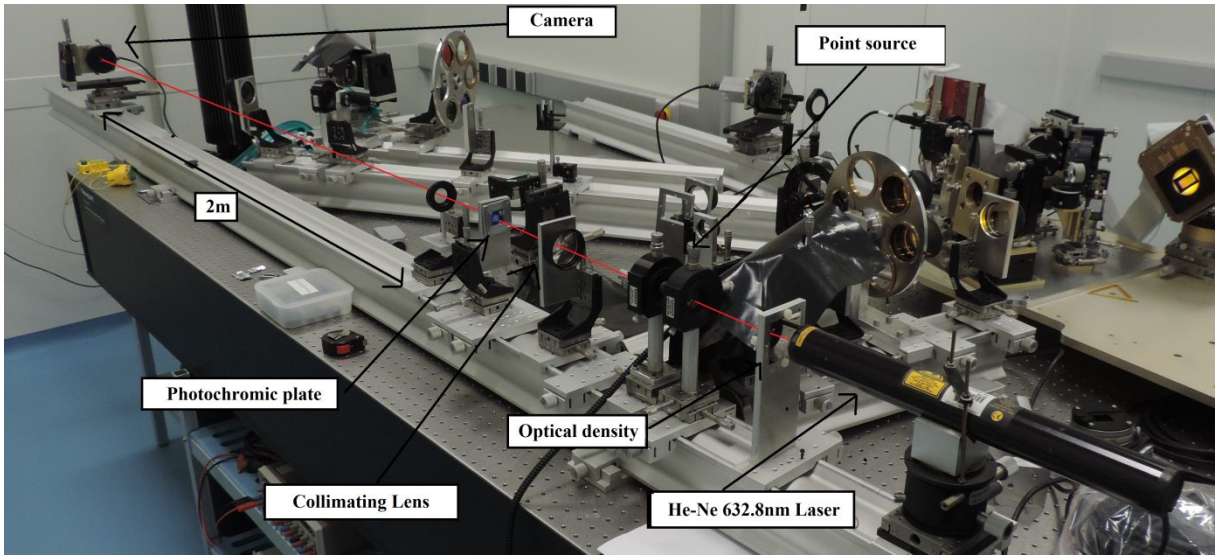

Figure 3: Picture of the set-up dedicated to image reconstruction; it is based on a He-Ne laser, the CGH plane and the camera located at the hologram projection distance (2m in this case)

4. BINARY CGHs

The first object to be recorded on the plate is the binary CGH of the letter "Z", formed on a 10x10 pixel grid as shown on Fig 4(a), with a physical size of 2x2mm^2 and calculated at a focus of 2m. As the photosensitive material does not fully cover the 1 inch square support plate, a maximum CGH dimension of 1cmx1cm has been fixed, which leads to a CGH resolution of 720x720 pixels. The physical dimensions of the "Z" are fixed as 1/5 of the CGH dimensions. The object, smaller than the CGH, is surrounded by the Fresnel lens pattern. With a longer CGH the resolution may become insufficient because the fringes on the corner will be too close.

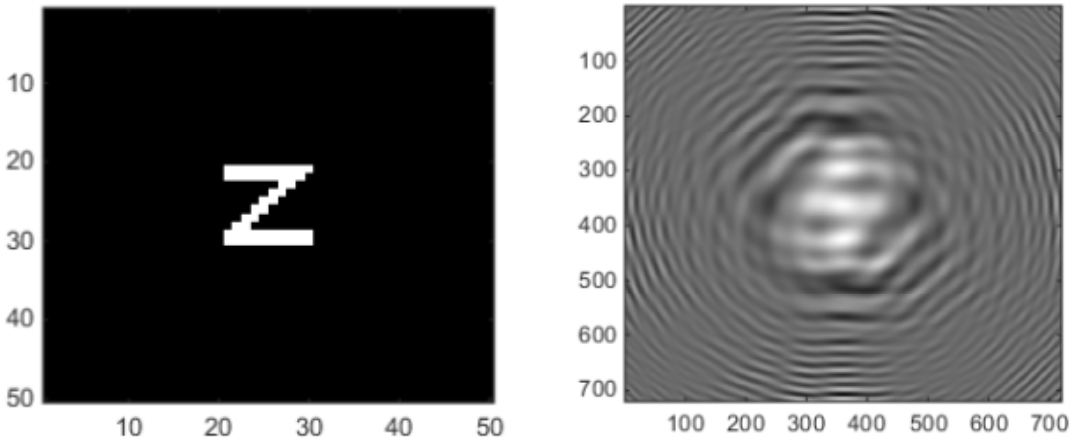

(a) *(b)*

Figure 4: (a) Original image to be encoded; a 10x10pixels "Z"
(b) 720x720 pixels calculated continuous CGH, for an image dimension of 2x2mm^2 at a focus of 2m

Usually, when the recording method is based on a physical mask or a laser, the CGH is binarized. Figure 5 represents the binary CGH obtained for our image, and the pattern recorded on the plate, and shows that it is a faithful reproduction. The vignetting effect seen on this image was due to the post-CGH imaging mount and has been corrected in the next paragraphs.

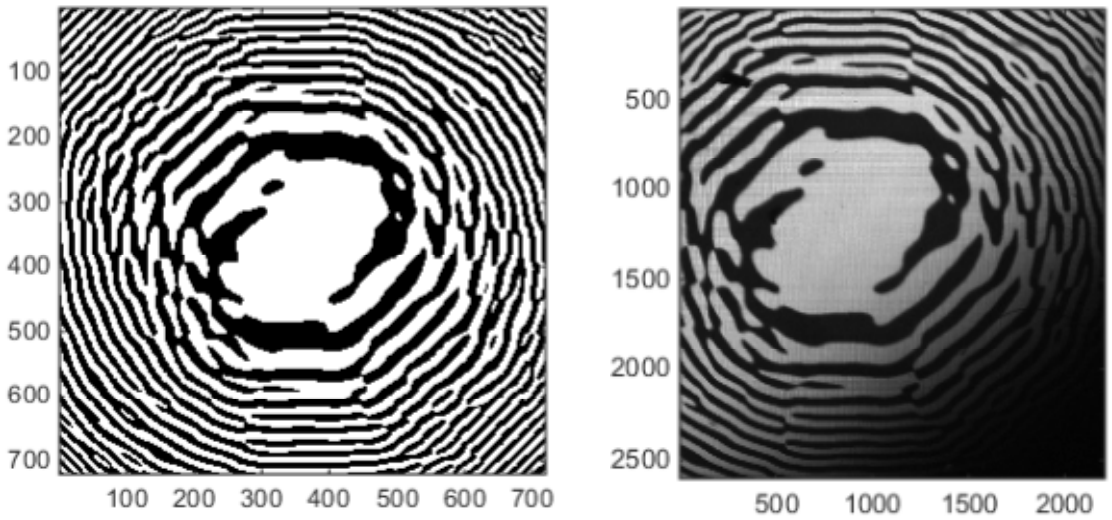

(a) *(b)*

Figure 5: (a) 720x720 pixels calculated binary CGH and (b) actual pattern recorded on the plate

We can also simulate the reconstructed image by applying the direct transformation of the binary Fresnel CGH, which allows us to check the reliability of the code.

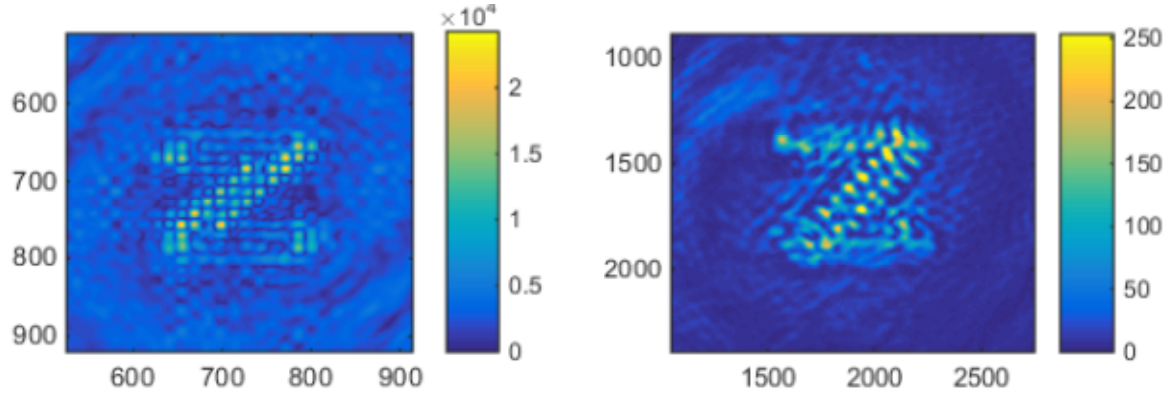

(a) *(b)*

Figure 6: Reconstruction of a 720x720 pixels CGH of a 10x10 pixels "Z" of 2x2mm at 2m : (a) Simulation and (b) Real reconstruction

In figure 6 is shown the reconstructed image, identical to the simulated one. It shows the quality of our recording and reconstruction set-ups.

However, the obtained image does not completely look like the original image (Fig. 4a). This is due to the fact that binary CGHs can only reconstruct pixilated images, because they do not suit well the shape of the calculated continuous CGH and then neglect some information.

5. STEPPED CGH

The advantage of our recording method is the ability to easily write grayscale CGHs, and then reconstructs not only pixilated images but fulfilled ones. Since the DMD is a programmable mask, it is possible to change the mask projected during recording, in order to expose each pixel the desired time and then create gray levels. But for this, we must first characterize the photochromic material time response.

5.1 Illumination law

As described in the introduction, the photochromic material becomes progressively transparent when illuminated by visible light. This means that a given level of transparency, i.e. a given level of gray, corresponds to a given exposure time. But the response of the material is not linear and has to be characterized. Our recording set-up could take images of the plate during the recording, thanks to the post-CGH camera. Therefore we enlightened the plate, and took images every 30 seconds to plot the photochromic plate time response shown in figure 7.

This curve, called illumination law, gives the transparency of the plate as a function of exposure time. Specifically, it is the illumination law that will be followed to finely control the transparency of the plate. This law has been obtained for a given light power, but it has been verified that it can be rescaled with a homothetic transformation in order to obtain the right illumination curve for another light power.

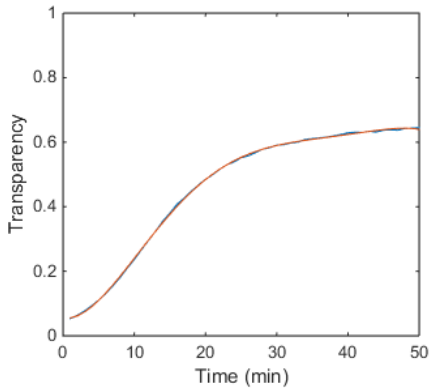

Figure 7: Illumination law of the photochromic plate

A binary CGH can easily be recorded with our set-up; it simply requires displaying it on the DMD and to project it on the plate during the required time. While recording a stepped CGH, a serial of binary mask has to be defined, with the adequate exposure time for each of them. We decided to discretize the CGH in 20 gray levels, this number of steps is sufficient as the difference between the continuous and stepped CGH falls then below 1%. Twenty binary masks are calculated by binarizing the continuous CGH pattern with thresholds ranging from 0 to 1 in steps of 0.05. Once the serial of mask obtained, each exposure time is deducted from the illumination law show in figure 7. The curve shown in figure 8 gives us the exposure time for each mask. They range from 1min 32sec up to 11min 43sec.

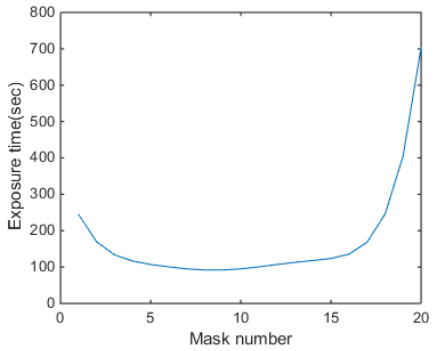

Figure 8: Exposure time of each mask when the CGH is stepped in 20 levels

5.2 Mask generation

Figure 9 illustrates the recording strategy using the example of a detail of the 10x10 pixels "Z" CGH. Each mask is displayed during its own exposure time to reach the following discrete level of transparency. We can see that the darker areas are illuminated with the first masks only, while the most transparent areas are illuminated through almost all masks. 20 masks have been calculating, the figure shows 7 of them with the theoretical stepped CGHs image where it is possible to identify them.

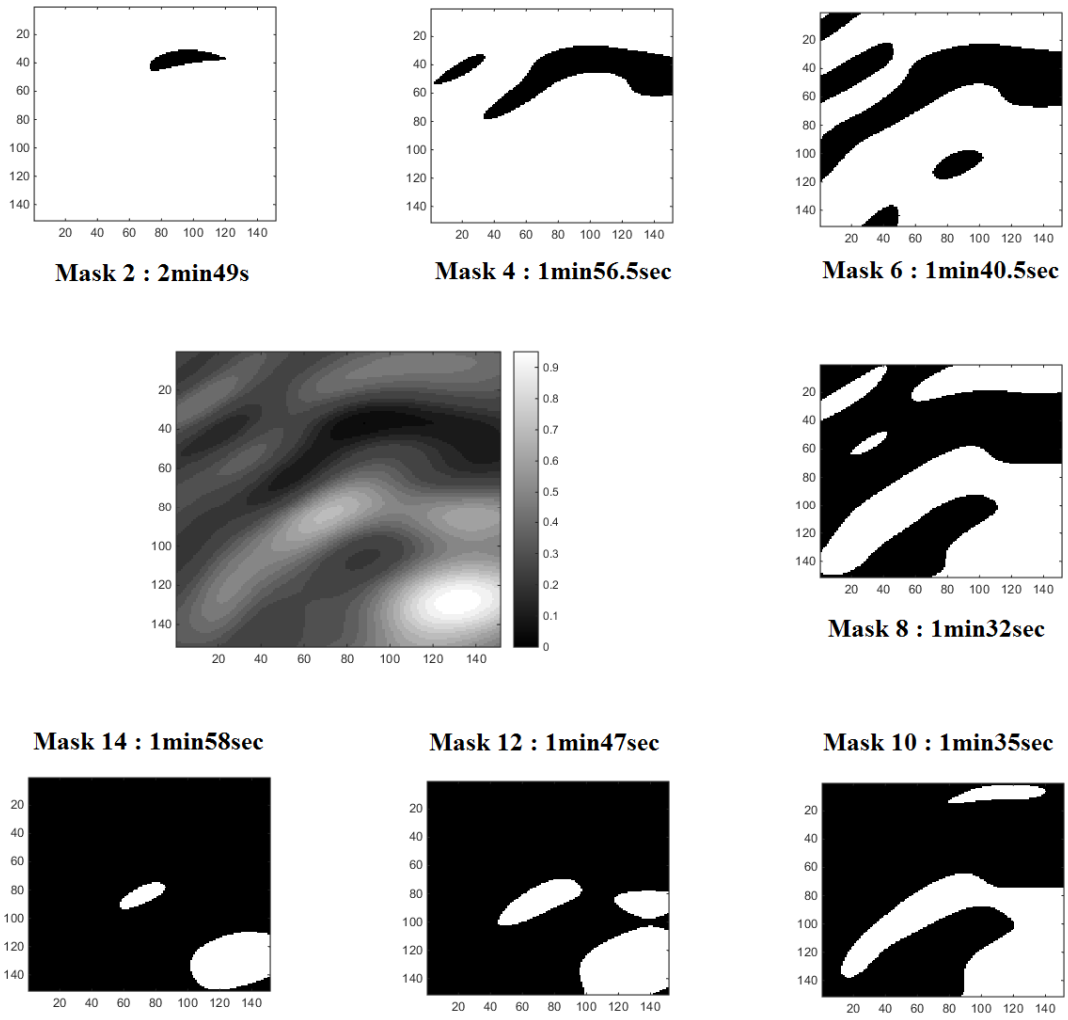

Figure 9: Recording strategy: detail of the CGH and the corresponding 7 masks out of the serial of 20 masks

This method has already been used on phase CGH but with a low quality result due to critical issues like the good alignment of successive masks. With a DMD, this problem obviously disappears since the position error between 2 consecutive masks is zero; in addition, it is instantaneous to apply the masks.

5.3 Stepped CGHs recording

We have been able, thanks to the method described above, to get the CGH on figure 10b. It corresponds to the CGH calculated for a 200x200 pixels "Z" of a size of 2x2mm located at 2m and stepped into 20 levels.

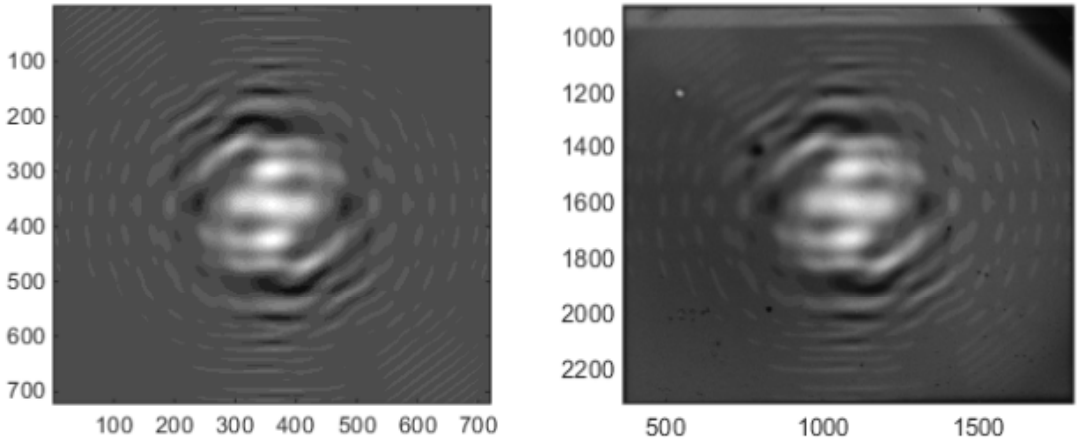

(a) *(b)*

Figure 10: 720x720 pixels stepped CGH, of a 200x200 pixels "Z" of 2x2mm at a focus of 2m: (a) calculated; (b) recorded

To be sure that the zones correspond to our expectations, the contours of the theoretical stepped CGH are displayed on the real one as shown in figure 11. It represents a small area of CGH, obtained with an optical magnification of 1:3.75; the contours (black lines) correspond to the limit between the level 7 and 8 in the theoretical CGH and it is exactly at the right place on the real one while red arrows show that even a single mirror shift is visible.

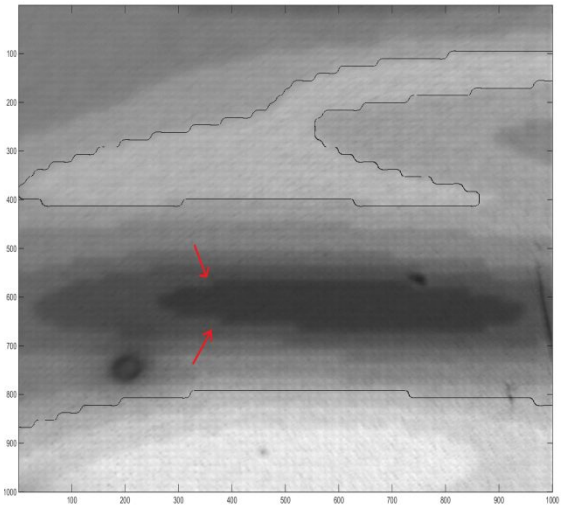

Figure 11 : Magnification of a part of the CGH written; with contours and arrows showing the resolution of the recording

Figure 11 shows the precision of our recording technique. Each micro-mirror is clearly identifiable and each zone is perfectly defined. The fact that the pattern of the DMD is visible on the plate could have been a source of additional noise, but after verification (both calculation and measurement) it has actually no measurable impact.

It would have been possible to remove this high frequency pattern with a *sub-pixel dithering* strategy. The principle is to slightly shift the plate at different positions during the exposure with a pitch smaller than a pixel. This technique allows smoothing the CGH, and then makes the high frequency pattern due to the DMD disappear.

5.4 Verification of illumination law

Figure 12 shows another detail of the actually recorded CGH, with respect to the corresponding zones on the calculated CGH. It has been imaged with an optical magnification of 1:3.75.

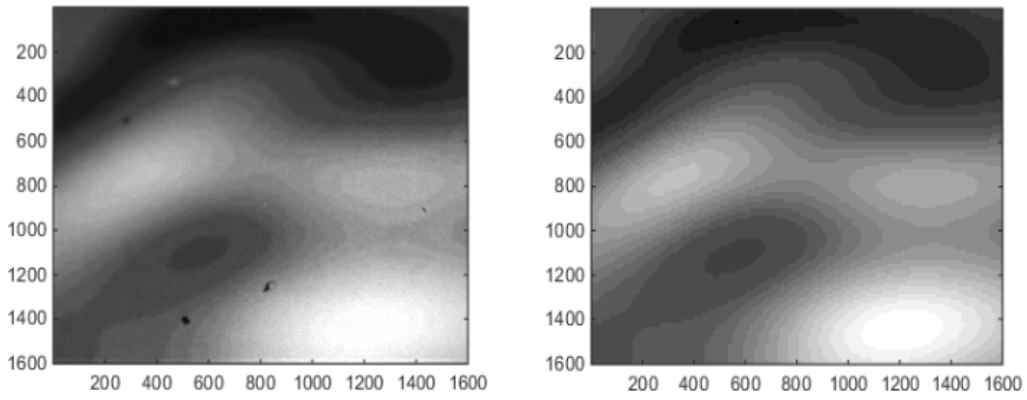

(a) *(b)*

Figure 12: 1600x1600 pixels area of the stepped CGH: (a) actual image of the recorded CGH (b) corresponding area on the calculated CGH

All levels are present in this picture, so it allows us to verify that our illumination law is well defined. The mean of each level has been calculated independently on pixels sample number larger than 10^5. The obtained curve is linear, with a standard deviation of 1.4%.

5.5 Stepped CGHs reconstruction

Figure 13 shows the simulated reconstructed image and the actual reconstructed image using our second set-up (paragraph 3.2). The image dimension on the camera is 570x570 pixels, which gives a physical size of 2x2mm as expected. Very faithful reconstruction has been obtained with respect to the simulated reconstructed image as well as the original 200x200 pixels "Z" image.

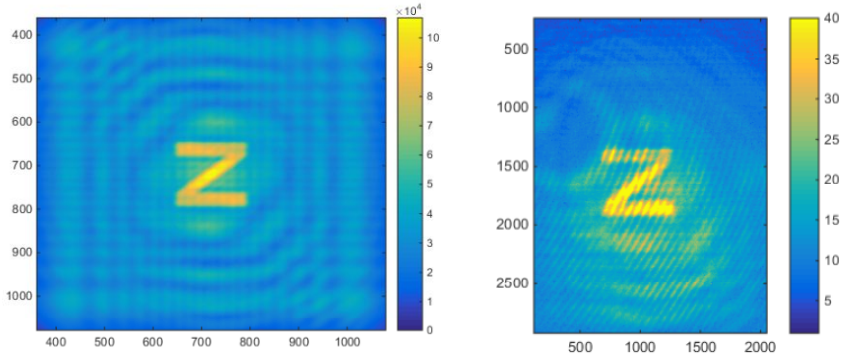

(a) *(b)*

Figure 13: Reconstruction of a 720x720 pixels stepped CGH, of a 200x200 pixels "Z" of 2x2mm at a focus of 2m
(a) Simulation of the reconstruction from theoretical CGH
(b) Real reconstruction of the image

A shadow appears on the upper left hand side of the experimentally reconstructed image, it corresponds to the diffraction caused by a defect on the CGH plate, visible in Figure 10b. Fresnel CGHs are very sensitive to defects and cannot be reconstructed correctly if the most transparent areas are altered. The image size and the focus chosen for the calculation also depend on the quality of the illumination. If the laser beam converges instead of being well collimated, the focus will be shorter and the size of the image smaller, and vice versa if the laser beam is diverging. Note also in figure 13b interference fringes probably due to multiple reflections in the plate itself.

5. CONCLUSION

Computer generated holograms are tools well suited for optical testing and wavefront shaping. But up to now amplitude holograms have only been recorded in binary format. Our method can increase the efficiency of this tool by enabling the realization of stepped holograms by generating discrete gray levels.

We have been able to successfully record several Fresnel CGHs, with stepped and binary coding. The resolution of recorded holograms was set to 720x720 pixels to be able to project it on the functional part of the photosensitive plate, up to 1x1 cm^2 size. The high optical resolution of our set-up allowed making high quality recorded CGH with the desired grayscale properly produced. The reconstructed images using stepped holograms are also very faithful to the original image without being pixilated as for binary holograms.

The next step will be to code wavefronts containing phase information. We also plan to conduct the same study on Fourier holograms because they are much faster to compute and may give better results according to preliminary simulations. Finally, we will also use our method to create apodizers, using the same protocol as for stepped CGHs.

ACKNOWLEDGMENTS

This work has been partly funded by the European Union FP7-OPTICON 2 program.

REFERENCES

[1] B R, Brown and A W, Lohmann, "Complex Spatial Filtering with Binary Masks," Appl. Opt; **5**, 967 (1966)
[2] A W, Lohmann and D P, Paris, "Binary Frauhnofer Holograms Generated by Computer," Appl. Opt. **5**, 1739 (1967)
[3] A. W. Lohmann, D. P, Paris, and H. W. Werlich, "A computer Generated Spatial Filter Applied to Code Translation," Appl. Opt. **6**, 1139 (1967)
[4] A. W. Lohmann and D. P. Paris, "Computer Generated Spatial Filters for Coherent Optical Data Processing," Appl. Opt. **7**, 561 (1968)
[5] J.J. Burch, "A Computer Algorithm for the Synthesis of Spatial Frequency Filters," Proc. IEEE **55**, 599–601
[6] W. H. Lee, "Sampled Fraunhofer Hologram Generated by Computer," J. Opt. Soc. Am. **58**, 729A (1968)
[7] L. B. Lesem, P. M. Hirsch and J. A. Jordan, Jr., "Generation of Discrete-point Holograms," J. Opt. Soc. Am. **57**, 1406A (1968)
[8] L. B. Lesem, P. M. Hirsch, and J. A. Jordan, Jr., "Computer Synthesis of Large-scale Holograms," J. Opt. Soc. Am. **57**, 1406A (1967)
[9] L.B. Lesem; P.M. Hirsch & J.A. Jordan, "The Kinoform: A New Wavefront Reconstruction Device," Journal of Research and Development (IBM) **13**, 150–155 (1969)
[10] L. Rosen, "Moiré Effects in Computer Generated Holograms," Proc. IEEE **55**, 1736 (1967)
[11] N. K. Sheridon, "Production of Blazed Holograms," Appl. Phys. Letters **12**, 316 (1968)
[12] J. P. Waters, "General Fourier Transform Method for Synthesizing Binary Holograms," J. Opt. Soc. Am. **58**, 729A (1968)
[13] S. Reichelt, C. Pruss, H. Tiziani, " Specification and characterization of CGHs for interferometrical optical testing ," Proc. SPIE Vol. **4778** (2002)

[14] C. Pruss, S. Reichelt, H. Tiziani, W. Osten, “CGH in interferometric testing,” Opt. Eng. **43**(11), 2534-2540 (2004)
[15] A.J. MacGovern and J.C. Wyant, “CGH for testing optical elements,” Applied optics Vol. **10** (619), (1971)
[16] Y-T. Lu, C-S. Chu, H-Y. Lin, “Characterization of the gray-scale photolithography with high-resolution gray steps for precise fabrication of diffrative optics,” Opt. Eng. **43**(11) 2666-2670 (2004)
[17] N. Luo, Y. Gao, S. He, Y. Rao, “Research on exposure model for DMD-based digital gray-tone mask ,” Proc SPIE Vol. **7657**, 7657 12-1 (2010)
[18] Frederic Zamkotsian, Paolo Spano, Patrick Lanzoni, Harald Ramarijaona, Manuele Moschetti, Marco Riva, et al., “BATMAN: a DMD-based Multi-Object Spectrograph on Galileo telescope” in Proceedings of the SPIE conference on Astronomical Instrumentation 2014, Proc. SPIE **9147**, Montréal, Canada, (June 2014)
[19] G. Pariani, C. Bertarelli, G. Dassa, A. Bianco, G. Zerbi, ”Photochromic polyurethanes for rewritable CGHs in optical testing,” Optics Express **5**, 4536 (2010)
[20] A. W. Lohmann and S. Sinizinger, “Graphic codes for computer holography,” Appl. Opt. **34**, 17 (1995)
[21] C. B. Burckhardt, “A simplification of Lee’s method of generating holograms by computers,” Appl. Opt. **9**, 1949-1959 (1970)
[22] C. K. Hsueh and A. A. Sawchuk, “Computer-generated double-phase holograms,” App. Pot. **17**, 3874-3883 (1978)
[23] L. Denis, PhD Thesis, “Traitement et analyse quantitative d'hologrammes numériques. Interface homme-machine,” Université Jean Monnet - Saint-Etienne, France (2006), hal.archives-ouvertes.fr/tel-00282661/
[24] F. Zamkotsian, E. Grassi, P. Lanzoni, R. Barette, C. Fabron, K. Tangen, L. Marchand, L. Duvet "DMD chip space evaluation for ESA EUCLID mission," in Proceedings of the SPIE conference on MOEMS 2010, Proc. SPIE **7596**, San Francisco, USA (2010)
[25] F. Zamkotsian, P. Lanzoni, E. Grassi, R. Barette, C. Fabron, K. Tangen, L. Valenziano, L. Marchand, L. Duvet " Successful evaluation for space applications of the 2048x1080 DMD," in Proceedings of the SPIE conference on MOEMS 2011, Proc. SPIE **7932**, San Francisco, USA (2011)
[26] J. W. Goodman, “Introduction to Fourier Optics,” Mc Gray-Hill (1996)